Experimental determination of the surface density for the 6He exotic nucleus

L. R. Gasques,[1] L. C. Chamon,[1] D. Pereira,[1] V. Guimarães,[1] A. Lépine-Szily,[1] M. A. G. Alvarez,[1] E. S. Rossi, Jr.,[1]
C. P. Silva,[1] B. V. Carlson,[2] J. J. Kolata,[3] L. Lamm,[3] D. Peterson,[3] P. Santi,[3] S. Vincent,[3] P. A. De Young,[4] and G. Peasley[4]

[1]*Laboratório Pelletron, Instituto de Física da Universidade de São Paulo, 05315-970 São Paulo, SP, Brazil*
[2]*Departamento de Física, Instituto Tecnológico de Aeronáutica, Centro Técnico Aeroespacial, São José dos Campos, SP, Brazil*
[3]*Physics Department, University of Notre Dame, Notre Dame, Indiana 46556*
[4]*Physics Department, Hope College, Holland, Michigan 49422*
(Received 2 May 2002; published 4 February 2003)

Angular distributions for the elastic scattering of 4,6He on 58Ni have been measured at near-barrier energies. The present data, combined with others for the 4He + 58Ni system at intermediate energies, allowed the determination of the 4,6He ground-state nuclear densities through an unfolding method. The experimentally extracted nuclear densities are compared with the results of theoretical calculations.

One of the most exciting recent events in nuclear physics has been the discovery of extended neutron distributions in exotic neutron-rich nuclei, such as, e.g., 11Li, 11Be, and 6,8He. The advent of facilities that produce radioactive ion beams made possible the search for experimental evidence of thick neutron skins and halos for nuclei near the drip line. This phenomenon was first observed by obtaining the interaction radii from reaction cross section measurements for systems involving exotic nuclei [1], followed by the experimental determination of transverse momentum distributions from the breakup products [2]. Several recent works with radioactive beams use the elastic scattering process at intermediate energies to demonstrate the existence of such extended neutron distributions. However, from a theoretical point of view, the near-barrier energy region should be more appropriate for studying the densities in the surface region, where the difference between exotic and neighboring stable nuclei is much more emphasized. In fact, for distances close to the barrier radius, the nuclear potential is mostly determined by the folding of the nucleon-nucleon interaction with the surface region of the densities. This idea has already been successfully applied to determine densities of stable nuclei [3–5]. Taking this point of view, we present elastic scattering differential cross sections for the 4,6He + 58Ni systems at near-barrier energies, with the aim of obtaining the 4,6He densities in the surface region. The analysis is extended to the 4He + 58Ni system at intermediate energies, and in this case information about the 4He density at much smaller distances is obtained.

The experiment was carried out at the Nuclear Structure Laboratory of the University of Notre Dame. The 6He secondary beam with $E_{Lab} = 9.0$ MeV was produced using the *TwinSol* radioactive ion beam facility [6]. In this system, two superconducting solenoids act as thick lenses to collect and focus the secondary beam onto the target. The 6He beam was produced using the proton transfer process of the 7Li primary beam at an energy of 19.95 MeV incident on a 12.7-μm-thick 9Be production target 9Be(7Li,6He). Ions with the same magnetic rigidity of the 6He were present in the secondary beam. The detection system was composed of four telescopes consisting of thin Si detectors (energy loss), backed by thicker Si detectors (remaining energy), making it

possible to identify particles with different charges and masses. A typical ΔE vs E spectrum for the 6He + 58Ni system is shown in Fig. 1(a). The elastic 6He group is clearly visible and scattered 4He ions can also be easily identified. In recent works [7,8], a strong 4He group resulting from transfer and/or breakup modes has been observed in the scattering of 6He on 209Bi in energies below the nominal Coulomb barrier. With the purpose of investigating the importance of such channels for the 6He + 58Ni system, we have also performed measurements for the 6He + 197Au system [see Fig. 1(b)], with the same secondary beam conditions as those for the 6He + 58Ni. For the 6He + 197Au system, the contributions arising from other reaction channels, besides the elastic scattering, are expected to be negligible, since the 9 MeV bombarding energy corresponds to about 10 MeV below the Coulomb barrier. Indeed, the elastic scattering cross section for this system is in agreement with the corre-
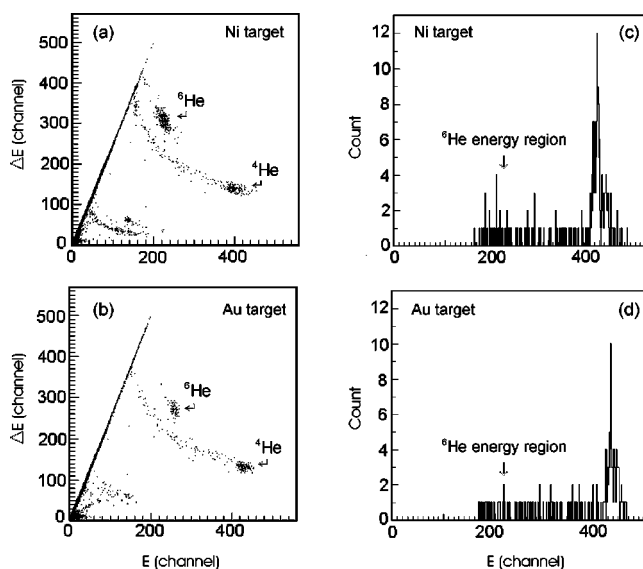

FIG. 1. Typical ΔE vs E spectra obtained using (a) 58Ni and (b) 197Au targets. The corresponding energy projections for the 4He ions are shown in (c) and (d), respectively. The arrows in (c) and (d) indicate the energy region that corresponds to the elastic scattering of the 6He.
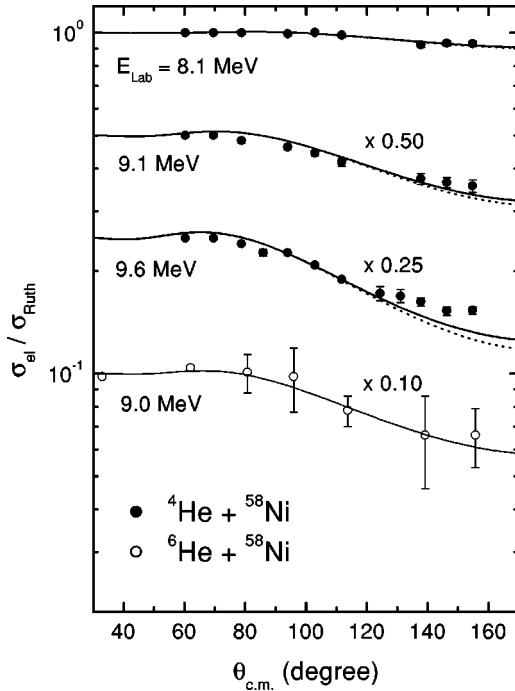
FIG. 2. Elastic scattering angular distributions for the ^{4,6}He $+ {}^{58}$Ni systems at several near-barrier energies. The lines represent optical model predictions with (solid lines) or without (dotted lines) considering the compound-elastic contribution.

sponding Rutherford cross section. The energy projection spectra corresponding only to ^{4}He ions are also shown in Figs. 1(c) and 1(d). The very similar background for both targets (^{197}Au and ^{58}Ni) indicates that no significant transfer and/or breakup contributions were present in our experiment. We estimate the contribution of these processes for the ^{6}He $+ {}^{58}$Ni system as less than 2% of the elastic scattering cross section, by comparing the ^{4}He background for both targets. As a result of the energy resolution of our experiment, any contribution of inelastic scattering to low-lying states is included in our "elastic scattering" data. The secondary beam of ^{4}He was produced in a similar way, but using the elastic scattering process of the ^{4}He primary beam. In this case, the secondary beam is much more intense than that for ^{6}He, since the cross section for elastic scattering is much greater than that for the transfer process. Figure 2 exhibits the elastic scattering cross section for the ^{4,6}He$+ {}^{58}$Ni systems at several near-barrier energies. Contributions to the count rate in the region of the elastic scattering process can also arise from the compound-elastic (CE) decay. Since this process is mixed (experimentally) with the elastic channel, in our analyses the Hauser-Feshbach theory has been used to estimate the CE cross section. We checked that the contribution of the CE cross section for the ^{4}He$+ {}^{58}$Ni system at intermediate energies and for the ^{6}He$+ {}^{58}$Ni system at the near-barrier region is negligible. Figure 3 exhibits the elastic scattering data (from Refs. [9–12]) for the ^{4}He$+ {}^{58}$Ni system at intermediate energies.

The extraction of information on nuclear densities from elastic scattering is a question of using the folding model for the interaction, including all the important effects from first
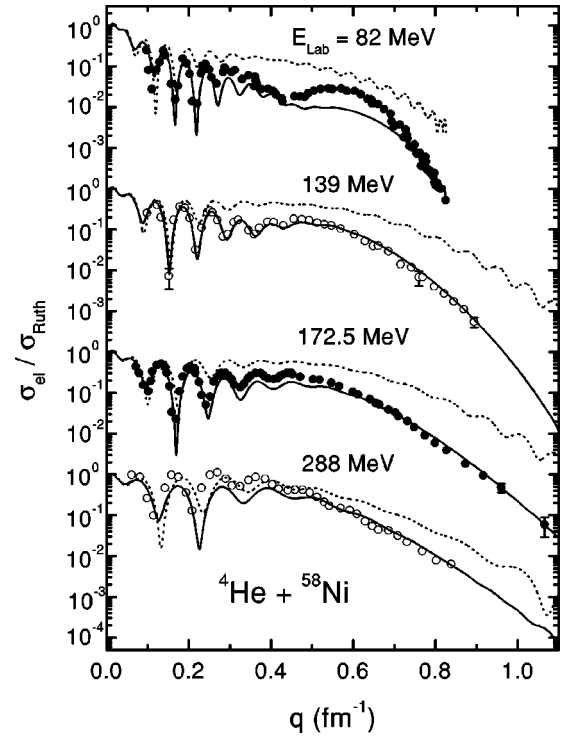

FIG. 3. Elastic scattering angular distributions as a function of the momentum transferred for the ^{4}He$+ {}^{58}$Ni system at several intermediate energies. The lines represent optical model predictions, in which the nonlocal model has been assumed for the real part of the interaction, with a Lax-type (dashed lines) or a Woods-Saxon shape (solid lines) for the imaginary part of the potential.

principles and avoiding the use of adjustable parameters as much as possible. In this work, we use a model for the real part of the potential that is based on nonlocal quantum effects related to the exchange of nucleons between the target and the projectile [13–16]. The nonlocal model has provided a good description of the elastic scattering for several systems in a very wide energy range [4,5,14–17]. It also has been successfully checked for inelastic scattering and transfer processes at subbarrier and intermediate energies [5,15–17]. We also point out that the nonlocal model has provided good predictions for a very extensive systematic of potential strengths extracted from heavy-ion elastic scattering data analyses at low and intermediate energies [13]. Within this model, the bare interaction is connected with the folding potential V_F through

$$V_N(R,E) \approx V_F(R) e^{-4v^2/c^2}, \tag{1}$$

where c is the speed of light and v is the local relative speed between the two nuclei,

$$v^2(R,E) = \frac{2}{\mu}[E - V_C(R) - V_N(R,E)]. \tag{2}$$

For the Coulomb interaction V_C, we have used the expression for the double sharp cutoff potential [18]. This procedure is important in calculating cross sections at intermediate

energies, in which the internal region of the potential is probed. The folding potential depends on the densities of the two partners in the collision,

$$V_F(R) = \int \rho_1(r_1) \ \rho_2(r_2) \ u_0(\vec{R} - \vec{r_1} + \vec{r_2}) \ d\vec{r_1} \ d\vec{r_2}, \quad (3)$$

where $u_0(\vec{R} - \vec{r_1} + \vec{r_2})$ is the "frozen" M3Y effective nucleon-nucleon interaction [13,15].

The imaginary part of the interaction used in our calculations has also been based on general assumptions. For the angular distributions at intermediate energies, we have used the imaginary part of the parameter-free Lax-type interaction, which is known to be quite appropriate in this energy region [19,20]. At near-barrier energies we have used a Woods-Saxon (WS) shape for the imaginary potential, with parameters that result in complete internal absorption from barrier penetration, but with small strengths in the surface region. Within these conditions, the results obtained for the experimental density values from the data analysis are quite insensitive to variations of the WS potential parameters. This result should be contrasted with the strong dependence on the imaginary part of the potential in the data analysis for the ^{6}He + ^{209}Bi system [7,8]. In that case, very large cross sections for transfer and/or breakup processes have been detected at subbarrier energies, and an imaginary potential that results in strong surface absorption was used in the elastic scattering data analysis. However, no significant transfer and/or breakup contributions were detected for the ^{6}He + ^{58}Ni system here, and possible inelastic contributions are already included in the "quasielastic" data. Thus, there are no extra significant peripheral reaction processes to be accounted for in the present case, and the use of optical potentials with strong surface absorption clearly would be a mistake in the present data analysis.

If the nonlocal model is assumed for the interaction and the density of one nucleus is known, an unfolding method can be used to extract the ground-state nuclear density of the other nucleus from the elastic scattering data analyses. The method has already been successfully applied in the experimental determination of densities for the ^{12}C and ^{16,18}O nuclei [3–5]. In the present paper we describe the method in a quite concise form, and we invite the reader to obtain further details of the method in a complete discussion presented in the references above. In the data analyses, we have used a theoretical Dirac-Hartree-Bogoliubov density for the ^{58}Ni nucleus [21], since the corresponding predictions for electron scattering cross sections are in very good agreement with the data [3,4]. This theoretical density was also assumed in the previous works for stable nucleus systems and the corresponding results obtained for the densities were quite satisfactory. For obtaining the ^{4,6}He densities, we have assumed the two-parameter Fermi (2pF) distribution to describe the ^{4,6}He densities. The diffuseness (a) and radius (R_0) were searched for the best data fits, with the ρ_0 parameter determined by the normalization condition. For each angular distribution, we have found a family of densities which give equivalent data fits. These densities cross at the sensitivity
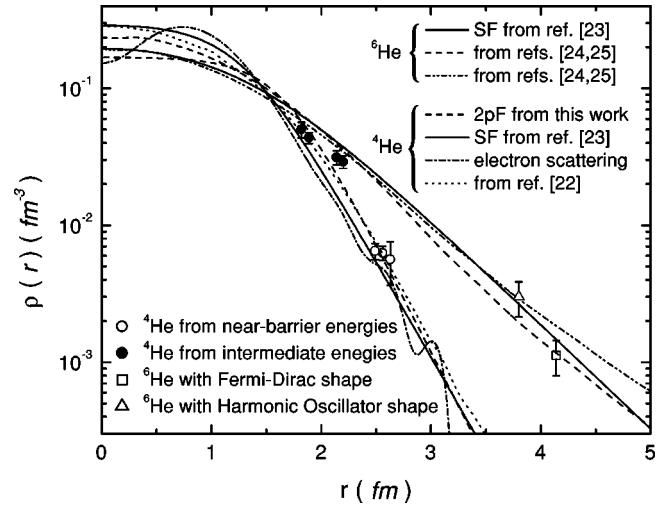

FIG. 4. Experimental nuclear density values at the sensitivity radii for the ^{4,6}He nuclei (open symbols), as obtained from near-barrier elastic scattering data analyses for the ^{4,6}He + ^{58}Ni systems. The solid symbols represent density values (^{4}He) from intermediate-energy data analyses, using the nonlocal model and the Lax-type interaction for the real and imaginary parts of the potential. Also presented in the figure are our best fit two-parameter Fermi (2pF) distribution for the ^{4}He, the experimentally extracted symmetrized Fermi (SF) distributions from Ref. [23], theoretical densities for the ^{4}He (Ref. [22]) and ^{6}He (Refs. [24,25]), and a total nucleon density for ^{4}He obtained from electron scattering experiments.

radius, where the value of the density is determined without ambiguity. To ensure that the sensitivity radius is in a region that is important to the data fits, we have used the notch test, in which a spline with a Gaussian shape is included in the ^{4,6}He densities, and the variation of the chi square is studied as a function of the position of this perturbation.

The sensitivity radius is energy dependent and therefore the density can be obtained over a large range of radial distances. Figure 4 contains the experimental nucleon density values for the ^{4,6}He at the corresponding sensitivity radii obtained from data analyses of several angular distributions. Information about the density at the surface region is obtained through the near-barrier elastic scattering data analyses, while the data at intermediate energies probe the density in the inner region. The statistical error bars for the density values have been determined using the procedure described in [4]. In earlier works [3,4], we have demonstrated for stable nuclei that the results obtained for the density values at the sensitivity radii are rather independent of the shape assumed for the density distribution. However, as ^{6}He is expected to be an exotic nucleus with an extended neutron tail, in the present work we have also used another shape to describe the ^{6}He density, the harmonic oscillator (HO) shape, with the aim of further checking the validity of our results. Figure 4 shows that the two models for the distribution result in sensitivity radii only slightly different (about 0.3 fm), with corresponding experimental density values compatible with the expected behavior (slope) of the ^{6}He density in the surface region. Actually, the dependence of the

experimental results on the model assumed for the distribution is expected to be weak, since the near-barrier data analysis is mostly sensitive to the surface region of the density, where any realistic model provides a shape close to an exponential (see the theoretical calculations for the ^{6}He density in Fig. 4). For intermediate-energy data analyses, besides the Lax interaction we have also used a Woods-Saxon shape imaginary potential with three free parameters, in order to evaluate any possible change in the sensitivity radius. The different models for the imaginary potential provide very similar results for the ^{4}He density.

The solid and dotted lines in Fig. 2 represent optical model predictions for the elastic scattering cross section, with (solid lines) or without (dotted lines) the CE contribution. For the ^{4}He+^{58}Ni system, these theoretical predictions were obtained by using the best fit 2pF distribution with $R_0 = 1.64$ fm and $a = 0.28$ fm (see Fig. 4). Figure 3 shows that the elastic scattering data fits using a Woods-Saxon shape for the imaginary potential are better than those obtained using the Lax-type interaction. Despite the differences in the elastic scattering data fits, we stress that both models for the imaginary part of the interaction provide very similar values for the density.

In this paper, we have studied the ^{4}He nucleus with the purpose of comparing the results for the ^{4}He and ^{6}He densities, and also with the aim of checking the validity of the method in this light mass region. Thus, in Fig. 4 we have compared our ^{4}He experimental density values with the total (proton+neutron) alpha density derived from the charge distribution obtained in ^{4}He electron scattering experiments. We have estimated the total distribution as twice the proton distribution. We have obtained the ^{4}He proton distribution (ρ_p) by unfolding the charge density of the nucleus (ρ_{ch}) with the intrinsic charge distribution of the proton in free space (ρ_{chp}),

$$\rho_{ch}(r) = \int \rho_p(\vec{r'}) \, \rho_{chp} \, (\vec{r} - \vec{r'}) \, d\vec{r'}, \qquad (4)$$

where ρ_{chp} is an exponential with diffuseness $a_{chp} = 0.235$ fm. In Fig. 4 we also present the results of theoretical calculations [22] for the ^{4}He nuclear density, which have been performed in the context of the generator coordinate method, with the Skyrme SIII nucleon-nucleon effective interaction and elimination of center of mass effects. We estimate the overall systematical error of our ^{4}He surface density values to be about 20%, by comparing our experimental results at the surface region with those from electron scattering and with the theoretical prediction. A similar estimate for systematical errors was already obtained in the previous works using the same method for the ^{12}C, ^{16,18}O stable nuclei [3,4].

We have obtained the ^{6}He experimental density (see Fig. 4) from the data analyses of the angular distribution for the ^{6}He+^{58}Ni system at $E_{Lab} = 9.0$ MeV. In Ref. [23], the ^{4,6}He nuclear densities were obtained from elastic scattering data analyses for the ^{4,6}He+ p systems at 700 MeV/nucleon, using the Glauber multiple scattering theory for the interaction. In that work, different parametrizations for the ^{6}He

density have been tested: symmetrized Fermi (SF) distribution, Gaussian with halo (GH), a Gaussian for the core, and two different models for the valence nucleons, Gaussian (GG) and $1p$-shell harmonic oscillator-type density (GO). All these distributions provided very similar density values (from data analyses) for the ^{6}He density in the radial distance region $0 \leq r \leq 5$ fm. For the purpose of comparison, the corresponding SF distributions for the ^{4,6}He nuclei are included in Fig. 4 (solid lines). The experimentally extracted densities of that work are in good agreement with our density values at the sensitivity radii, in spite of the very different energies, systems, and assumptions of the two works.

In Fig. 4, we also show two theoretical calculations (from [24,25]), using Faddeev wave function models, for the ^{6}He density. These models incorporate different n-n and n-p potentials with variation of the two-neutron binding energy. The different shapes (2pF or HO) assumed for the distribution in the present work provide results for the ^{6}He density that approach both theoretical calculations at different sensitivity radii (see Fig. 4). Thus, the statistical and systematical errors of our method do not allow one to distinguish which theoretical calculation for the ^{6}He is better. However, the good agreement between experimental and theoretical results is evident, corroborating that the effect of the two extra neutrons of the ^{6}He greatly increases the density at the surface region in comparison with that of the ^{4}He nucleus.

In Ref. [13], with the aim of systematizing the heavy-ion nuclear densities for stable nuclei, we have calculated theoretical distributions for a large number of nuclei using the Dirac-Hartree-Bogoliubov model. We have determined that the average value for the density diffuseness is 0.50 fm and the dispersion associated with this value, due to effects of the structure of the nuclei, is about 0.025 fm. The value for the diffuseness of the exotic ^{6}He, obtained from the theoretical calculations [24,25] (see Fig. 4), is about 0.65 fm, very far from the average value for stable nuclei. Within this context, we could also say that the ^{4}He is an eccentric nucleus, since the corresponding 2pF and SF distributions (see Fig. 4) provide $a \approx 0.3$ fm.

In summary, in this work we have obtained experimental density values in the surface region for the ^{4,6}He nuclei from low-energy data analyses. The assumptions of the method have been fully discussed and several checks of the results have been provided. The parameter-free real part of the interaction used in this work contains as basic inputs just the well-known M3Y effective nucleon-nucleon interaction and our model for the Pauli nonlocality, which has been extensively tested. Also the imaginary part of the interaction has been based on very general assumptions: the lack of surface absorption at low energies and the parameter-free Lax type interaction, which is known to be quite appropriate for intermediate energies. We have also determined statistical and systematical errors for the experimental density values. The systematical errors arise from several possible sources: the dependence of the position of the sensitivity radius on the shape assumed for the projectile distribution, the theoretical density assumed for the target, the contribution of the real part of the polarization potential that arises from nonelastic couplings, which has not been included in our analysis, etc.

The value of about 20% obtained for the systematical error in the ^{4}He case is very similar to those found for other nuclei in previous works. Thus, we consider that the systematical error for the ^{6}He should also be about 20%, or even somewhat greater because in this case the effect of the reaction channels on the real part of the polarization might be more significant. Therefore, efforts to decrease cross section data uncertainties would not be very useful in the present case. Even so, for purpose of comparison between the ^{6}He and ^{4}He densities, this systematical error ($\approx 20\%$) is actually not very significant, because at the surface region the ^{6}He density is about two orders of magnitude greater than that for ^{4}He. Finally, within the precision of the method, our experimentally extracted result for the ^{6}He density in the surface region is in very good agreement with theoretical predictions, and it is also compatible with other experimental results obtained under quite different conditions in a previous work.

---

[1] I. Tanihata *et al.*, Phys. Lett. **160B**, 380 (1985).

[2] T. Kobayashi *et al.*, Phys. Rev. Lett. **60**, 2599 (1988).

[3] M. A. G. Alvarez, E. S. Rossi, Jr., C. P. Silva, L. R. Gasques, L. C. Chamon, D. Pereira, M. N. Rao, B. V. Carlson, C. De Conti, R. M. Anjos, P. R. S. Gomes, J. Lubian, S. Kailas, A. Chatterjee, and P. Singh, Phys. Rev. C **65**, 014602 (2002).

[4] L. R. Gasques, L. C. Chamon, C. P. Silva, D. Pereira, M. A. G. Alvarez, E. S. Rossi, Jr., V. P. Likhachev, B. V. Carlson, and C. De Conti, Phys. Rev. C **65**, 044314 (2002).

[5] E. S. Rossi, Jr., D. Pereira, L. C. Chamon, C. P. Silva, M. A. G. Alvarez, L. R. Gasques, J. Lubian, B. V. Carlson, and C. De Conti, Nucl. Phys. **A707**, 325 (2002).

[6] M. Y. Lee, F. D. Becchetti, T. W. O'Donnell, D. A. Roberts, J. A. Zimmerman, V. Guimarães, J. J. Kolata, D. Peterson, P. Santi, P. A. De Young, G. F. Peaslee, and J. D. Hinnefeld, Nucl. Instrum. Methods Phys. Res. A **422**, 536 (1999).

[7] E. F. Aguilera, J. J. Kolata, F. M. Nunes, F. D. Becchetti, P. A. De Young, M. Goupell, V. Guimarães, B. Hughey, M. Y. Lee, D. Lizcano, E. Martinez-Quiroz, A. Nowlin, T. W. O'Donnell, G. F. Peaslee, D. Peterson, P. Santi, and R. White-Stevens, Phys. Rev. Lett. **84**, 5058 (2000).

[8] E. F. Aguilera, J. J. Kolata, F. D. Becchetti, P. A. De Young, J. D. Hinnefeld, Á. Horváth, L. O. Lamm, Hye-Young Lee, D. Lizcano, E. Martinez-Quiroz, P. Mohr, T. W. O'Donnell, D. A. Roberts, and G. Rogachev, Phys. Rev. C **63**, 061603(R) (2001).

[9] H. H. Chang, B. W. Bridley, T. M. Braid, T. W. Colon, E. F. Gibson, and N. S. P. King, Nucl. Phys. **A270**, 413 (1976).

[10] D. A. Goldberg, S. M. Smith, H. G. Pugh, P. G. Roos, and N. S. Wall, Phys. Rev. C **7**, 1938 (1973).

[11] J. Albinski, A. Budzanowski, H. Dabrowski, Z. Rogalska, S. Wiktor, H. Rebel, D. K. Srivastava, C. Alderlieste, J. Bojowald, W. Oelert, C. Mayer-Böricke, and P. Turek, Nucl. Phys. **A445**, 477 (1985).

[12] B. Bonin, N. Alamanos, B. Berthier, G. Bruge, H. Faraggi, J. C. Lugol, W. Mittig, L. Papineau, A. I. Yavin, J. Arvieux, L. Farvacque, M. Buenerd, and W. Bauhoff, Nucl. Phys. **A445**, 381 (1985).

[13] L. C. Chamon, B. V. Carlson, L. R. Gasques, D. Pereira, C. De Conti, M. A. G. Alvarez, M. S. Hussein, M. A. Candido Ribeiro, E. S. Rossi, Jr., and C. P. Silva, Phys. Rev. C **66**, 014610 (2002).

[14] M. A. Cândido Ribeiro, L. C. Chamon, D. Pereira, M. S. Hussein, and D. Galetti, Phys. Rev. Lett. **78**, 3270 (1997).

[15] L. C. Chamon, D. Pereira, M. S. Hussein, M. A. Cândido Ribeiro, and D. Galetti, Phys. Rev. Lett. **79**, 5218 (1997).

[16] L. C. Chamon, D. Pereira, and M. S. Hussein, Phys. Rev. C **58**, 576 (1998).

[17] M. A. G. Alvarez, L. C. Chamon, D. Pereira, E. S. Rossi, Jr., C. P. Silva, L. R. Gasques, H. Dias, and M. O. Roos, Nucl. Phys. **A656**, 187 (1999).

[18] R. M. Devries and M. R. Clover, Nucl. Phys. **A243**, 528 (1975).

[19] M. S. Hussein, R. A. Rego, and C. A. Bertulani, Phys. Rep. **201**, 279 (1991).

[20] R. J. Glauber, *Lectures in Theoretical Physics* (Interscience, New York, 1959), Vol. 1, p. 315; *High-Energy Physics and Nuclear Structure* (Plenum, New York, 1970), p. 207.

[21] B. V. Carlson and D. Hirata, Phys. Rev. C **62**, 054310 (2000).

[22] D. Galetti, M. A. Talarico, and A. F. R. de Toledo Piza (unpublished).

[23] G. D. Alkhazov *et al.*, Phys. Rev. Lett. **78**, 2313 (1997).

[24] J. S. Al-Khalili, J. A. Tostevin, and I. J. Thompson, Phys. Rev. C **54**, 1843 (1996).

[25] M. V. Zhukov, D. V. Fedorov, B. V. Danilin, J. S. Vaagen, J. M. Bang, and I. J. Thompson, Nucl. Phys. **A552**, 353 (1993).